Local field potentials, BOLD and spiking activity – relationships and physiological mechanisms

Philipp Berens[1,2,3], Nikos K. Logothetis[1,4], Andreas S. Tolias[2,5,6]

1 Max Plank Institute for Biological Cybernetics, Tübingen, Germany

2 Baylor College of Medicine, Houston, USA

3 Werner Reichardt Centre for Integrative Neuroscience and Institute for Theoretical Physics, University of Tübingen, Tübingen, Germany

[4]Division of Imaging Science and Biomedical Engineering, University of Manchester, Manchester, M1 7HL, UK.

[5]Michael E. DeBakey Veterans Affairs Medical Center, Houston, TX 77030, USA.

[6]Department of Computational and Applied Mathematics, Rice University, Houston, TX 77005, USA.

Extracellular voltage fluctuations (local field potentials, LFPs) reflecting neural mass action are ubiquitous across species and brain regions. Numerous studies have characterized the properties of LFP signals in the cortex to study sensory and motor computations as well as cognitive processes like attention, perception and memory. In addition, its extracranial counterpart – the electroencephalogram – is widely used in clinical applications. However, the link between LFP signals and the underlying activity of local populations of neurons is still largely elusive. For the LFP to aid our understanding of cortical computation, however, we need to know as precisely as possible what aspects of neural mass action it reflects. In this chapter, we examine recent advances and results regarding the origin, the feature selectivity and the spatial resolution of the local field potential and discuss its relationship to local spiking activity as well as the BOLD signal used in fMRI. We place particular focus on the gamma-band of the local field potential since it has long been implicated to play an important role in sensory processing. We conclude that in contrast to spikes, the local field potential does not measure the output of the computation performed by a cortical circuit, but are rather indicative of the synaptic and dendritic processes, as well as the dynamics of cortical computation.

Neural ensembles represent information about the sensory world, cognitive processes or motor plans in the patterns of their action potentials. These patterns result from computations performed on the inputs to a local circuit and combine various sources of feedforward or feedback information as well as modulatory signals. Every cortical pyramidal cell receives approximately 10,000 synaptic inputs, about 75% of which are excitatory, the exact numbers varying between structures and species (Abeles, 1991; Braitenberg and Schüz, 1998). The vast majority of these excitatory inputs arise from other cortical neurons, each presynaptic cell providing only a few synapses. The strong convergence of synaptic input onto each cortical cell shows the degree of integration at the single-cell level and gives us an indication of the complexity of the computations performed at each recording site. These computations ultimately determine the properties of the canonical cortical microcircuit, which is thought to be the elementary processing unit of cortex (Douglas and Martin, 1991, 2004).

One important approach to gain insight into the computational and dynamical properties of neural ensembles is by recording the action potentials of a large number of neurons simultaneously (Csicsvari et al., 2003a; Buzsáki, 2004; Tolias et al., 2007). Such techniques are crucial to our understanding of the resulting representation after cortical processing and to study precisely how individual cells contribute to it. To fully understand the computation performed within a cortical microcircuit, however, it is important to monitor precisely which

synaptic inputs an individual neuron receives and how these signals are integrated on its dendritic tree to result in its spiking output. While we do not yet have the means to study these processes with the necessary precision in vivo in individual cells, the local field potential (LFP) has been hypothesized to provide an aggregate signature of the synaptic input and dendritic processing within a localized cortical network (Mitzdorf, 1987; Logothetis, 2003). For the LFP to aid our understanding of cortical computation, however, we need to know as precisely as possible what aspects of neural mass action it reflects. In this chapter, we examine recent advances and results regarding the origin of the local field potential and discuss its relationship to local spiking activity as well as the more global BOLD mechanisms used in fMRI. We place particular focus on the gamma-band of the local field potential since it has long been implicated to play an important role in sensory processing. In addition, we concentrate on data from the visual cortex of awake macaques, but point to relevant literature from other systems where appropriate. The chapter is based on our recent reviews on these matters (Logothetis, 2008; Berens et al., 2008a).

Physiological mechanisms of the local field potential

An extracellular electrode placed in the brain measures the mean extracellular field potential, comprised of the aggregate electrical activity generated by various neural processes in a cell ensemble around the electrode tip (Figure 1A). For instance, the high frequency range (from 0.6–1 to 3 kHz) of this signal has been estimated to carry a signature of the spiking activity of up to a few thousand cells located within a radius of 140–300 μm around the electrode tip (Gray et al., 1995; Henze et al., 2000; Logothetis, 2008). It is referred to as multi-unit (MU) activity and can be seen as reflecting the output of a local neural population.

Figure 1 about here

In contrast, low frequency voltage fluctuations (<200 Hz) represent a different aspect of neural mass action: Local field potentials (LFP) are commonly thought to be related to perisynaptic processes on the dendrites, that is, excitatory or inhibitory postsynaptic potentials (Mitzdorf, 1985, 1987). They are believed to originate from a weighted average over potential changes in the vicinity of the electrode tip, generated by current sinks and sources in extracellular space (as reviewed by Logothetis, 2003, 2008; Berens et al., 2008a). These are generated, for instance, when synchronous excitatory synaptic input activates the dendrites of a neuron, leading to a current sink at the dendrite and a source at the soma (Figure 1C; Mitzdorf, 1985; Nunez and Srinivasan, 2006). The resulting dipole contributes to the measured LFP depending on the arrangement of the generating cell with respect to the local population. For example, pyramidal cells have large dendritic arbors facing in one direction opposing their somata and their dendrites are neatly aligned with each other [a so-called "open field arrangement" (Johnston and Wu, 1995)]. Therefore, processes on the dendrites of pyramidal cells in the cortex are thought to contribute strongly to the LFP, as potential differences within the local network do not cancel each other due to their geometrical arrangement (Figure 1D). The signature of action potentials in the extracellular electric field is commonly thought to occur at frequencies above 500Hz, however, and therefore it is believed that spikes likely do not directly add to the LFP power. Nevertheless, some authors believe that low frequency components of spike waveforms or a superposition of waveforms might 'contaminate' the LFP (Pesaran et al., 2002; Liu and Newsome, 2006; David et al., 2010). Regardless, local spiking may to some extent

be reflected in the LFP as it will generate synaptic potentials via local excitatory connections on nearby pyramidal cells. While it was originally thought that excitatory postsynaptic potentials are the primary source of LFP generating dipoles (Mitzdorf, 1985, 1987), more recently also other sources have been found to contribute significantly to the LFP such as inhibitory synaptic input (Hasenstaub et al., 2005; Trevelyan, 2009; see also below), and integrative soma-dendritic processes including subthreshold membrane oscillations (Kamondi et al., 1998) and afterpotentials of somatodendritic action potentials (Buzsáki, 2002). In addition, simulations have shown that not all synaptic potentials have the same influence on the LFP, but that their impact may vary with the position of the active synapse and the position of the recording electrode (Linden et al., 2010).

Figure 2 about here

Oscillators contributing to the LFP at different frequencies are possibly generated by processes on varying scale and strength (Buzsaki and Draguhn, 2004; Logothetis et al., 2007). Low frequency oscillations, on the one hand, may arise in thalamocortical feedback loops giving rise to strong slow oscillators and are thought to be modulated by global neuromodulatory inputs (Steriade et al., 1993; Steriade, 2006). Gamma-rhythms, on the other hand, most likely originate locally within cortical microcircuits consisting of pyramidal cells and interneurons (Figure 2; Mann et al., 2005; Fries et al., 2007; Logothetis, 2008; Cardin et al., 2009; Sohal et al., 2009). Such generators may be identified by a combination of biophysical modeling and the application of statistical techniques such as Independent Component Analysis (Makarov et al., 2010). The most striking characteristic of these cortical neural networks is recurrence. Some axonal collaterals of the pyramidal cells ascend back to and synapse in superficial layers, while others distribute excitation in the horizontal plane (Lund et al., 1994), forming a strongly recurrent excitatory network (Douglas and Martin, 2004). Interposed between this pyramidal network is a large variety of inhibitory, GABAergic interneurons (Markram et al., 2004). Inhibitory interneurons can receive both excitatory and inhibitory synapses onto their somata and have only local connections. About 85% of them in turn innervate the local pyramidal cells. Different types of inhibitory interneurons are capable of targeting different subdomains of neurons, i.e. dendritic regions, somata, or axons (DeFelipe, 1997). For example, basket cells [about 50% of all inhibitory neurons in cortex (Markram et al., 2004)] target the somata and proximal dendrites of pyramidal cells and are therefore excellent candidates for the role of gain-adjustment of the integrated synaptic response (Pouille et al., 2009). Chandelier cells, on the other hand, target the axons of nearby neurons and can completely override all the complex dendritic integration and somatic gain settings by "choking" the action potential output at the last moment (e.g. Miles et al., 1996; Zhu et al., 2004).

Experimentally, recurrent activity in such networks has been shown to be the source of the gamma-oscillations in the hippocampus of rats (Csicsvari et al., 2003b), where pyramidal cells and interneurons form networks with a distinct spatial layout much like in cortical tissue. Similarly, we postulate that microcircuits in cortex get activated by thalamic input and recurrent processing loops between pyramidal neurons of layer 4 and 2/3 and interneurons then generate gamma-oscillations commonly observed during visual stimulation (Figure 3, see below). Thus, while pyramidal neurons may be the strongest mediator of dipoles contributing to the LFP due to their size and geometry, interneurons play an important role in generating the dipoles underlying gamma-oscillations: They act as rhythm generators via rhythmic inhibition of pyramidal neurons and synchronized

inhibitory synaptic potentials contribute significantly to the membrane oscillations on pyramidal neurons (Whittington et al., 1995; Hasenstaub et al., 2005; Bartos et al., 2007; Fries et al., 2007). For a more detailed discussion of interneuron networks and their role for cortical gamma-oscillations, see the reviews by McBain and Fisahn (2001), Bartos et al. (2007) and Fries et al. (2007).

Figure 3 about here

Direct evidence for a causal role of inhibitory interneurons comes from recent experiments using optogenetic manipulations of cortical circuitry in mouse cortex (Cardin et al., 2009; Sohal et al., 2009). Cardin et al. used channelrhosopsin to selectively activate either fast-spiking interneurons or regular-spiking pyramidal cells. When stimulating inhibitory interneurons with light pulses at frequencies in the gamma-range, they found a prominent increase in LFP gamma power, which could not be induced by stimulation of pyramidal cells. Further, Sohal et al. found that deactivating fast-spiking interneurons using halorhodopsin effectively blocks gamma-oscillations (Sohal et al., 2009). In addition, driving these interneurons by means of photostimulation with non-rhythmic pyramidal cell activity is sufficient to create gamma oscillations, providing further evidence for the importance of fast-spiking interneurons.

The interplay between pyramidal cell and interneuron networks can give rise to network oscillations in the gamma-band similar to those observed in the LFP even when individual neurons do not show oscillatory firing behavior. Theoretical work by Brunel and Wang has shown that oscillations in the gamma-range naturally emerge despite low firing rates and weakly structured firing rates in individual neurons when reciprocal connections between pyramidal cell and interneuron populations are present (Brunel and Wang, 2003). In this case, the observed network frequency depends strongly on the balance between excitatory and inhibitory currents, as pyramidal-to-interneuron connections and the pyramidal-to-pyramidal connections tend to decrease the population frequency. While the work of Brunel and Wang studied the population spike count and thus not the LFP itself, Mazzoni et al. used a model network consisting of sparsely and randomly connected leaky integrate-and-fire neurons with one excitatory and one inhibitory population and simulated the generation of the LFP from excitatory and inhibitory synaptic currents (Mazzoni et al., 2008). Interestingly, even such a simple model without the fine-structure of cortical microcircuits reproduced quantitatively accurate the dependence of LFP gamma-power on stimulus contrast as well as the dependence of information content in different LFP bands measured under naturalistic stimulation in V1 (see below). Recently, Kang et al. studied a mean-field rate model of the synaptic conductance rate in a reduced model of V1, which takes the major features of the functional organization of V1 into account (Kang et al., 2010). In particular, this model contains thalamic input as well as feedback from extrastriate cortex in addition to the well studied excitatory-inhibitory circuits within V1. The authors find that under visual stimulation such a network exhibits resonant behavior – that is, it starts to oscillate – in the gamma-band and point to extrastriate feedback as an important determinant of the exact oscillatory frequency of the network. In addition to such reduced models, detailed biophysical modeling will likely help to further untangle the importance of different contributions to the LFP (Makarov et al., 2010; Pettersen et al., 2008).

Local Field Potentials in the Visual Cortex

In different brain areas, the LFP comes in widely different flavors. In the hippocampus, for instance, strong theta oscillations between 4 and 10 Hz are the most prominent feature. They are believed to be critical for temporal coding of information and synaptic plasticity in these circuits (Buzsáki, 2002), as well as hippocampal–cortical interactions (Siapas et al., 2005; Sirota et al., 2008). In awake primates, sensorimotor regions of the cortex exhibit pronounced oscillations in the beta frequency band between 15 and 30 Hz related to motor preparation and planning (Sanes and Donoghue, 1993; Scherberger et al., 2005). Finally, in primary visual cortex of awake primates fast oscillations in the gamma-band between 30 and 90 Hz are dominant during visual stimulation (Figure 1B, e.g. Frien et al., 2000; Berens et al., 2008b). These gamma-oscillations are often subdivided in low-gamma oscillations (30–70 Hz) and high-gamma oscillations (> 70 Hz, often including frequencies well above 100 Hz). They are implicated to arise during cortical computations underlying visual processing, attention and other cognitive functions, reflecting the interplay between neuronal connectivity and neuronal dynamics. For a more general overview of the role of gamma-rhythms, see Fries (2009).

It is important to appreciate the rich phenomenology of different modulations that can occur in the local field potential, most likely as a result of the physiological processes contributing and the local circuit architecture: Local spiking activity affects mostly the gamma-band, while neuromodulatory processes affect predominantly low frequencies (<15 Hz, Steriade, 2006). The term "the LFP" is often used in a rather loose way and, frequently, results obtained using, e.g., the raw and the gamma-filtered LFP trace are directly compared. We believe that the different components of the LFP need to be understood at a sufficient level of detail before they can be used to draw inferences about microcircuit mechanisms. We will focus in this chapter on the properties of the gamma-band of the LFP in the visual cortex and touch on the properties of other frequency regimes only occasionally.

In the absence of visual stimulation, the LFP in the primary visual cortex of awake macaques is dominated by slow fluctuations (Figure 3A), such that the power in low frequencies dominates the frequency spectrum (Figure 3B; .e.g. Young et al., 1992; Juergens et al., 1999; Henrie and Shapley, 2005; Berens et al., 2008b) and the frequency spectrum shows approximately a power-law behavior (Bedard et al., 2006) . This frequency dependence of the LFP power spectrum is likely not due to a frequency dependence of the impedance spectrum since the impedance of the cortical tissue has been found to be isotropic and independent of frequency (Ranck Jr, 1963; Logothetis et al., 2007): Logothetis et al. measured the impedance spectrum in monkey visual cortex in the tangential plane at varying depths (Figure 4) and found no evidence for capacitive properties of the cortical tissue proving strong evidence that the impedance of cortical tissue is indeed frequency independent (but see Bédard and Destexhe, 2009). However, even in purely resistive extracellular medium the morphology of neural dendrites may result in a low-pass filtering effect on neural oscillations and thus frequency dependent attenuation (Linden et al., 2010; Pettersen and Einevoll, 2008).

Figure 4 about here

Dominant fast oscillations in the gamma-band (30–90 Hz) emerge during visual stimulation (Figure 3A) and we observe, accordingly, a pronounced increase of the power in this band (Figure 3C, for review, see Berens et al.,

2008a). While at the beginning of each trial a large stimulus evoked transient is present, gamma-oscillations clearly dominate its later part. Interestingly, enhanced gamma-power has been observed in different visual areas during processes like perception (Gail et al., 2004; Wilke et al., 2006), memory (Pesaran et al., 2002) and attention (Fries et al., 2001, 2008; Taylor et al., 2005). These gamma-oscillations show pronounced structure across cortical layers: They are stronger in the more superficial layers 1-4 than in the deep layers 5 and 6 and a sharp coherence transition occurs below layer 4 (Maier et al., 2009). Spikes of single neurons occur preferentially at the trough of these oscillations ("phase-locking", e.g. Fries et al., 2001; Berens et al., 2006; Ray et al., 2008b; Vinck et al., 2010). This phase-locking mechanism may play an important role in neural coding and might enable synaptic plasticity (Fries et al., 2007; Nadasdy, 2009; Masquelier et al., 2009; Lee et al., 2009). In particular, more strongly excited cells may fire earlier in the gamma-cycle, such that the relative strength of the external drive is recoded in the phase of the spike relative to the gamma-cycle. Some evidence for this has recently been reported in the visual cortex (Vinck et al., 2010). In any case, gamma-power is the single most relevant feature for the prediction of spike density functions from the LFP (Rasch et al., 2008). Recent evidence suggests that a quadratic non-linearity may improve the ability to predict spike rates from gamma-power significantly (Mazzoni et al., 2010). The coupling between spikes and LFP under visual stimulation as measured by the frequency dependent spike-field coherence is also highest in the gamma-band (Siegel and Konig, 2003). Together, this evidence corroborates the idea that LFP gamma-power originates in cortical microcircuits from processes that are linked to the spiking of local populations of cortical neurons and, as gamma-oscillations occur predominantly during visual stimulation, they reflect the ongoing computations in these networks.

Feature selectivity of the LFP in V1

The feature selectivity of local groups of neurons such as measured by MU activity has been mapped extensively – especially in primary visual cortex – and for many features the spatial organization of MU preferences is well known (e.g. Hubel and Wiesel, 1974; Bartfeld and Grinvald, 1992; Blasdel, 1992a, 1992b; Ringach et al., 1997; Lund et al., 2003). One extensively studied feature of neurons in visual cortical areas is their orientation tuning. In primary visual cortex, most MU sites respond with an elevated firing rate to bars or gratings of a certain orientation (Hubel and Wiesel, 1968; Ringach et al., 2002) and show a Gaussian-like tuning profile around this preferred orientation. It is natural to ask whether this important characteristic of neurons in V1 is also present in the gamma-band of the LFP recorded in this area. Indeed, the LFP gamma-power increases in a stimulus specific manner during visual stimulation with an oriented grating (Frien et al., 2000; Kayser and König, 2004; Berens et al., 2008b). Furthermore, its selectivity for stimulus orientation was stronger for the gamma-band in comparison to any other frequency band of the LFP. Nevertheless, even this most strongly tuned LFP band is less selective for orientation than MU activity measured simultaneously at the same site (Frien et al., 2000; Berens et al., 2008b).

To further compare the feature selectivity of the two signals, we also compared orientation tuning curves of the average LFP power in the gamma-band and the corresponding MU spiking responses recorded from the same tetrode. We chose the gamma-band for this analysis because this was the frequency band with highest stimulus selectivity (Berens et al., 2008b). Interestingly, at some sites the preferred orientations of both signals agreed well

while at others they did not, and differences in preferred orientation were widely distributed. The overall correlation between preferred orientations obtained from the gamma-band of the LFP and the MU activity recorded simultaneously was surprisingly low (~0.2; Berens et al., 2008b). We believe that this difference may be partly due to the different spatial sampling profiles of LFP and MU activity (see below). Consistent with this hypothesis, sites with smaller differences between the preferred orientations of the two signals also had higher orientation selectivity in the gamma-band, possibly reflecting a more homogenous region of the orientation map (see Figure 6D in Berens et al, 2008b). When we analyzed how the correlation between the preferred orientations of MU activity and LFP power changed as a function of frequency band, we found that it increased from its initial low values in the gamma-band to saturate over 150 Hz at ~0.8 (keep in mind, however, that less sites are tuned over all in these high-gamma band and mean selectivity is lower than in the low gamma-band). Possibly, this may be due to low-frequency components of local spiking activity contaminating the high-frequency bands of the local field potential (see above) or the fact that these high-frequency bands reflect the activity in more localized oscillators, which are faster but weaker.

The presence of ocular dominance columns is also a prominent feature of the organization of the primary visual cortex and typically cover slabs of about 500 μm in diameter (Hubel and Wiesel, 1968, 1974; Blasdel, 1992a). By selectively presenting stimuli to one eye only, we showed that the correlation between the ocular preferences of the MU activity and those of the LFP gamma-power is much higher than between their orientation preferences (~0.6; Berens et al., 2008b). Moreover, LFP and spiking activity also differ in their contrast response curves (Henrie and Shapley, 2005). For both signals, the response amplitude is enhanced with increasing contrast, but while many neurons show pronounced saturation in their firing rate at high contrasts, the gamma-power from the same site can still increase beyond this saturation point. Interestingly, the peak oscillation frequency in V1 increases linearly with increasing stimulus contrast (Ray and Maunsell, 2009).

In addition to differences in their orientation or contrast tuning, the gamma-band of the LFP and MU activity in primary visual cortex show different surround suppression characteristics (Gieselmann and Thiele, 2008). MU activity was typically maximal when the grating used for stimulation just covered its classical receptive field (CRF), and decreased when it was enlarged further. The gamma-power of the LFP, however, increased with grating size beyond the CRF. The maximal increase in oscillatory drive per unit area contributing to the LFP power occurred when stimuli covered approximately 0.5° of the receptive field surround. Interestingly, stimulation of the surround alone was not sufficient to evoke gamma-oscillations but stimulation of the CRF was required. In addition, there is some evidence that the stimulus size also determines the exact location of the peak in the power spectrum (Kang et al., 2010).

Belitski et al. studied how natural movies affect the properties of LFP spectra in V1 and found a prominent increase in LFP gamma power (Belitski et al., 2008) also during more naturalistic stimulation. Furthermore, they calculated the mutual information between the visual stimulus and the power in different LFP bands. Most information was contained in very slow (< 8 Hz) oscillations and the gamma-band at frequencies larger than 40 Hz. At high gamma frequencies above 70 Hz the LFP carried information about the stimulus which was very similar to MU activity, i.e. the two signals showed high signal correlations (~0.6). At low gamma frequencies, like those found to be most tuned to orientation in our study, this correlation was substantially weaker (~0.2-0.4).

Taken together, there is evidence that the LFP gamma-band and MU activity in primary visual cortex behave similarly in some circumstances, for example when probed for ocular dominance or – at high frequencies – information about natural movies. Importantly, the two signals seem to carry differing information regarding other features such as orientation tuning, spatial integration or contrast tuning. They are also differentially modulated by cognitive factors like attention (Chalk et al., 2010). We believe that these differences in response properties can be attributed partially to at least two key issues which we will discuss in turn: first, the LFP integrates signals from a larger area when compared to MU activity; second, the LFP reflects different aspects of cortical microcircuit activity than MU activity.

Feature selectivity of the LFP in other visual areas

The feature selectivity of the LFP gamma-band has also been measured in other visual areas. In area MT, Liu and Newsome have compared the direction and speed tuning of simultaneously recorded LFP and MU activity (Liu and Newsome, 2006). They found that the LFP is well tuned for both, direction and speed, and furthermore, that the tuning properties of an LFP site are well correlated with its MU tuning. Interestingly, Liu and Newsome report that tuning for preferred direction is nearly perfectly correlated between the two signals for frequencies larger than 40 Hz, while speed tuning shows only moderate correlation up to 110 Hz. In area V4, oscillations in the gamma-range have been related to the successful allocation of attention (Fries et al., 2001; Taylor et al., 2005). In area IT, the evoked response of local field potentials has been shown to be selective for object categories at roughly fifty percent of the studied sites, largely independent of the specific size or retinal location of the object (Kreiman et al., 2006). For MU activity, this number is much larger (~77 %). Interestingly, the LFP object preferences are poorly correlated with those of the MU activity (~0.2), but this correlation increases when spiking activity from up to 5 mm from the recording electrode is pooled. In comparison to the evoked response of the LFP, only ~25% of the studied sites showed object selectivity in the gamma-band. Similar to the visual cortex, feature selectivity of the LFP has also been studied in auditory (Kayser et al., 2007), somatosensory (Ray et al., 2008b, 2008a), parietal (Scherberger et al., 2005) and motor cortex (Rickert et al., 2005).

The spatial scale of the LFP

While for spiking activity relatively precise estimates of the volume from which spikes are recorded are available (140–300 mircometers; Gray et al., 1995; Henze et al., 2000; Logothetis, 2003, 2008), the experimental evidence regarding the exact spatial extent of the neural population contributing to the LFP remains somewhat contradictory. Partly, the perceived discrepancies stem from the fact that different studies report different measures of extent.

Estimates based on spectral coherence or correlation between simultaneously recorded sites (Destexhe et al., 1999; Juergens et al., 1999; Goense and Logothetis, 2008) or current-source density analysis (Mitzdorf, 1987) range from 500 μm up to several millimeters. Generally, low-frequency oscillations seem to be correlated over longer distances than high-frequency oscillations. For example, Goense and Logothetis (2008) report the distance at which the half-maximum of coherence-to-distance functions is reached. These show a coupling

region of 1.94 mm for low-gamma and 1.32 mm for high-gamma. Recent work by Rasch et al. (2009) in V1 and Kreiman et al. (2006) in IT supports this claim as MU spikes more than 1 mm away can successfully be used to predict the LFP.

We have taken a slightly different approach to estimating the spatial resolution of the LFP. Based on the poor correlation between the preferred orientations of MU activity and LFP gamma-band power and the high correlation between their ocular preferences, we hypothesized that this might be due to the differing spatial scales of the underlying feature maps in cortex. Orientation tuning of spiking activity is organized at a very fine spatial scale in macaque V1, where orientation columns span about 50 μm (Hubel and Wiesel, 1968, 1974, 1977). Ocular dominance columns, on the other hand, extend over about an order of magnitude more (Blasdel, 1992a; Hubel and Wiesel, 1968, 1977). The fact that the preferred orientations of MU activity and the LFP gamma-band are not well correlated but ocular dominance properties are suggests that the LFP gamma-band integrates signals over an area much larger than the size of orientation columns in V1. We therefore conjectured that the gamma-band of the LFP reflects signals integrated from an area with a radius at least 250–500 μm [note that in our original publication (Berens et al. 2008b) we reported diameter, not radius]. In line with our results, the correlation between MU activity and LFP gamma-band in MT in terms of speed tuning, which is organized on a spatial scale of 300–600 μm, is fairly high (Liu and Newsome, 2006). In addition, Liu and Newsome report a near perfect correlation between the two signals when looking at direction of motion tuning curves. Direction of motion is believed to be represented in MT on a similar spatial scale as orientation tuning in V1. The discrepancy to our study may either be explained by the differing stimulus size used or by the fact that LFPs to some extent also reflect the input into an area and neurons in V1 projecting to MT already show pronounced direction tuning (see below). A somewhat higher estimate on the spatial scale is provided by the study of Gieselmann and Thiele (2008) on the center-surround properties of LFP and MU in V1. Converting the radius of a grating driving the LFP most strongly via the cortical magnification factor to cortical distance, they concluded that the gamma-band of the LFP integrates sources as far as 0.6–1.2 mm away from the electrode tip.

Two more recent studies place the spatial resolution of the LFP more closely to that of MU activity. Katzner et al. recorded local field potentials from a multi-electrode array in cat primary visual cortex, which was implanted at a site where they had mapped out the orientation map beforehand using optical imaging (Katzner et al., 2009). They used a two-dimensional Gaussian weighting profile to predict the orientation tuning of the LFP from the map and found that the standard deviation of the optimal weighting profile was on the order of 100 μm, independent of whether event-related potentials or gamma-power were studied. They concluded that the spatial resolution thus must be on the order of 250 μm, since 2.5 standard deviations capture roughly 95% of the mass in the two dimensions of the orientation map. Xing et al. reached a very similar conclusion by measuring the receptive fields of evoked local field potentials using sparse noise stimuli (Xing et al., 2009). In addition, they estimated the local cortical magnification factor using an array of electrodes aligned in a linear track. Using this method, they find that the LFP arises from a local region with radius ~250 μm on average with clear laminar variation and a minimum in layer 4B of 120 μm.

Together, these results indicate that it is likely that in many instances measurements of the local field potentials reflect fairly local processes in the cortex, integrating signal sources from a few hundred micrometers of

surrounding tissue. This estimate is also corroborated by a recent biophysical modeling study (Pettersen et al., 2008), which finds the contribution to the LFP to arise predominantly from a region with radius up to 500 μm. In this study, the spatial profile of MU activity decayed more rapidly than that of the LFP, implying that the LFP might yet sample its signal from a somewhat larger region than MU activity. High correlation or coherence between sites farther apart may then originate from spatially distributed oscillators, which share common properties, such as common input from a neuromodulatory source for slow rhythms (Steriade et al., 1993; Steriade, 2006), a common thalamic driver or shared feedback connections for fast oscillations (Levitt and Lund, 2002; Angelucci and Bressloff, 2006; Angelucci and Sainsbury, 2006). In this way, the spatial resolution of the LFP measurement and the spatial extent of the stimulus may interact: a small stimulus possibly optimized in size for MU activity at the recording site will only activate a small network and the measured feature selectivity of the LFP may be biased towards recurrent activity generated only by a few cells with very homogenous properties. Gamma-power increases, however, with increasing stimulus size beyond the receptive field of MU activity (Gieselmann and Thiele, 2008), indicating that non-optimally driven cells or interneuron networks engaged by larger stimuli can also significantly contribute to the LFP. This is also corroborated by theoretical considerations, which highlight the importance of extrastriate feedback engaged by stimuli of different sizes (Kang et al., 2010).

It is important to note that the above studies have used widely different recording electrodes, ranging from high-impedance electrodes to multi-electrode Utah arrays and low-impedance wire-tetrode arrays, as well as used different referencing techniques. The effect of these differences has not been investigated systematically but is likely to affect the LFP properties and its spatial resolution. In the future, more realistic large-scale biophysical models (Pettersen et al., 2008; Linden et al., 2009, 2010) will likely help to clarify how the spatial resolution of the LFP is affected by different properties of the cortical microcircuit and under which conditions the current experimental estimates hold.

What does the LFP measure?

The low gamma-range of the LFP and MU activity show various dissociations with regard to their stimulus response properties (see above) and, in addition, their time courses can be strikingly different (Logothetis et al., 2001; Nir et al., 2007). While part of this finding may be explained by a larger integration radius of the LFP, the different signal sources reflected in the LFP in addition to spiking activity may contribute significantly to explain the observed differences as well. As outlined above, the LFP is constituted by synaptic events and other somato-dendritic processes occurring during recurrent cortical processing in a local microcircuit. To some extent, the signals arising during processing may have other feature tuning properties than the results of the computation, the spikes. In addition to recurrent activity in excitatory-inhibitory or excitatory-excitatory processing loops, the input to a microcircuit as well as feedback projections provide additional LFP signal sources (see above). While we have discussed excitatory-inhibitory feedback loops at length above, we will mention evidence for signatures of the latter two components in the following.

Swadlow and colleagues have used simultaneous recordings in the rabbit thalamus and barrel cortex to map the effect of thalamic spikes on cortical field potentials (Swadlow et al., 2002). Using laminar depth electrodes and raw LFP traces, they revealed a striking source-sink profile following thalamic spikes, with the major current sink

located in layer 4 lasting for 2-3 milliseconds and additional sinks located in layer 6. This clearly demonstrates that the input to an area can directly cause postsynaptic dipole patterns, whose sum is reflected in the local field potential. Additional functional evidence for a strong relationship between LFP power and input signals comes from a recent study in MT (Khawaja et al., 2009). Khawaja et al. recorded local field potentials as well as spiking activity in area MT while showing a plaid stimulus containing two gratings with differing but fairly close directions of motion. Many neurons in MT show pattern-selectivity in response to this stimulus, i.e. they respond most strongly if the average direction of motion is aligned with their preferred direction. In contrast, most V1 neurons show component-selectivity and respond most strongly if one of the directions of motion is aligned with their preferred direction. Interestingly, most LFP sites showed component-selectivity in the low gamma-band, very similar to that of V1 neurons. The authors suggest that this may be due to the fact that the LFP measures predominantly the input to MT provided by V1 neurons. If this is true, this may to some extent also explain the weak orientation tuning observed in V1 gamma-power and the low correlation between its preferred orientations and those of MU activity (Berens et al., 2008b). LGN cells in the macaque often exhibit a weak, but significant orientation tuning and preferred orientations are not uniformly distributed across the population, but rather cluster specific orientations depending on their receptive field location (Smith et al., 1990; Xu et al., 2002; but see the discussion of Berens et al., 2008b). Similar to the feedforward input to an area, the dendritic potentials caused by feedback projections likely also contribute significantly to the LFP. For V1, the importance of extrastriate feedback in explaining the dependence of the LFP spectrum on stimulus size has been highlighted in a recent modeling study (Kang et al., 2010). Furthermore, the effect of cognitive phenomena like attention and perceptual binding on the power of gamma-band oscillations demonstrates that higher-order feedback can contribute significantly to the LFP (for reviews, see Varela et al., 2001; Fries, 2009).

A shortcoming of the LFP is its inherent ambiguity. A change in the power of LFPs may reflect changes in the driving or feedback input, or changes in the baseline activity of a cortical microcircuit. As most of the excitatory input into an area arises locally from other pyramidal cells, LFPs will also indirectly reflect some of the postsynaptic effects of pyramidal cell activity. In addition, LFPs have a certain class bias, which in this case is determined by geometry and regional architecture. As described above, the open-field arrangement of the pyramidal cells will give rise to large LFP modulations; in contrast, synaptic potentials occurring on interneurons will contribute only weakly because of their star-shaped dendrites and their ataxic organization. Finally, inhibitory synapses may occasionally act as "shunts" for the excitatory currents through low-resistance channels, in which case large synaptic conductance changes may produce little effect in the membrane potential, and the precise location of a synaptic potential on the dendritic tree can influence its impact on the LFP. In summary, the LFP is a complex signal which may provide important clues about integrative processes not accessible otherwise. However, due to its nature it is unlikely to lead to a complete understanding of cortical processing and computation by itself. For this task, more precise techniques for monitoring different information sources independently are needed.

Relationship of neural signals to BOLD

Some of the current interest in local field potentials comes from their relationship with the BOLD signals, used

in functional imaging studies (fMRI). This relationship was examined directly in concurrent electrophysiology and fMRI experiments in the visual system of anaesthetized (Logothetis et al., 2001) and alert (Goense and Logothetis, 2008) monkeys. Initially, both LFPs and spiking seemed to be correlated with the BOLD response, although quantitative analysis indicated that LFPs are better predictors of the BOLD response than multiple-unit or single-unit spiking. The decisive finding leading to the papers' conclusion, however, was not the degree of correlation between the neural and the fMRI responses or the differential contribution of any type of signal into the BOLD responses, but rather the striking, undiminished haemodynamic responses in cases where spiking was entirely absent despite a clear and strong stimulus-induced modulation of the field potentials (Logothetis et al., 2001; Goense and Logothetis, 2008). Cortical sites, for instance, exhibiting strong neural response adaptation were characterized by MUA that returned to baseline a few seconds after stimulus onset, and LFPs that remained elevated for the entire duration of the visual stimulus (Figure 5). In this case, the LFP may potentially be generated by active interneuron networks which prevent pyramidal neurons from spiking but generate synaptic potentials and metabolic demand. Interestingly, the correlation between BOLD and LFP is highest, when the band-limited power in the gamma frequency range is examined (Kayser et al., 2004; Niessing et al., 2005).

Figure 5 about here

Differential contributions of LFP and MUA to the BOLD response can also be demonstrated with neuropharmacological manipulations permitting the selective modulation of interneuronal and pyramidal activity (Logothetis, 2003; Rauch et al., 2008). After the injection of 5HT, a profound suppression of the MU activity was observed. The LFP signal showed a slight increase and returned to baseline within a few minutes. However, no significant change was discernible in the BOLD response. Spectrograms obtained before and after the 5HT injection during visual stimulation showed that the stimulus-induced spikes were entirely eliminated, whereas LFP activity was moderately increased and the BOLD response remained unaltered (Logothetis, 2003; Rauch et al., 2008). In an elegant experiment, Viswanathan and Freeman used a dual microelectrode to conduct simultaneous and co-localized measurements of tissue oxygen and electrical activity at a high spatiotemporal resolution (Viswanathan and Freeman, 2007). Their experiments revealed a strong coupling between LFPs and changes in tissue oxygen concentration in the absence of spikes. They created this dissociation by exploiting well-known properties of the early visual system (for a detailed discussion of their findings, see Logothetis, 2007). Similar dissociations as described above had been demonstrated earlier between spikes and cerebral blood flow, which is closely related to the BOLD signal, in a number of elegant microstimulation studies in the cerebellum of rats, reviewed by (Lauritzen and Gold, 2003).

Despite this evidence for the role of perisynaptic activity in haemodynamics much discussion still concentrates on the importance of the firing rate of action potentials in the generation of the haemodynamic responses. Persistent assumptions about the relationship of spikes to neuroimaging signals might stem from the fact that for decades the important studies of neural correlates of behavior took the mean spiking rate to be the gold standard for quantifying neuronal activation. Given our current knowledge, local field potentials and, thus, to some extent the BOLD signal may instead be thought of as reflecting more the integrative processes instantiated in synaptic and dendritic activity than the spiking activity per se. Note that some aspects of the BOLD signal may not be related to neuronal processes at all: Sirotin and Das identified an anticipatory component of the

haemodynamic signal which could not be reliably predicted from either LFP or MU activity (Sirotin and Das, 2008). For a detailed review about the possibilities and limitations of fMRI and the BOLD signal, see (Logothetis, 2008).

Conclusions

In this chapter, we have reviewed the nature of LFPs as indicators of integrative processes in cortical microcircuits. In contrast to spikes, they do not measure the output of the computation performed by a cortical circuit, but are rather indicative of the synaptic and dendritic processes, as well as the dynamics of cortical computation. Oscillations in these potentials have been observed at various frequencies, but oscillations in the gamma-range between 30 and 90 Hz are most prominent in cortical areas. These oscillations most likely stem from fairly local sources, reflect to some extent input to a cortical circuit and intracortical processing in excitatory–inhibitory feedback loops and show interesting selectivity for many features commonly studied in visual areas, often dissociated from the preferences of the local spiking activity. It is the power of precisely these oscillations which is also best correlated with the BOLD signal measured by fMRI.

While fMRI alone is unlikely to reveal the actual mechanistic aspects of cortical circuit computation, it is an excellent tool for studying the global functional organization of cortical circuits (Logothetis, 2008). In conjunction with microstimulation (Tolias et al., 2005), it may be used to identify functionally connected subregions as has recently been done for the face patch system (Moeller et al., 2008). Subsequently, local field potentials and spiking activity may allow to gain a better understanding of the input–output transformation taking place within the regions, when their complimentary information is combined with the appropriate data analysis tools (Besserve et al., 2010; Panzeri et al., 2008; Magri et al., 2009; Gerwinn et al., 2009; Kelly et al., 2010; Murayama et al., 2010). An integrative approach to population coding in neural circuits makes use of all these signals and tries to put their individual strengths to optimal use.

Figure Captions

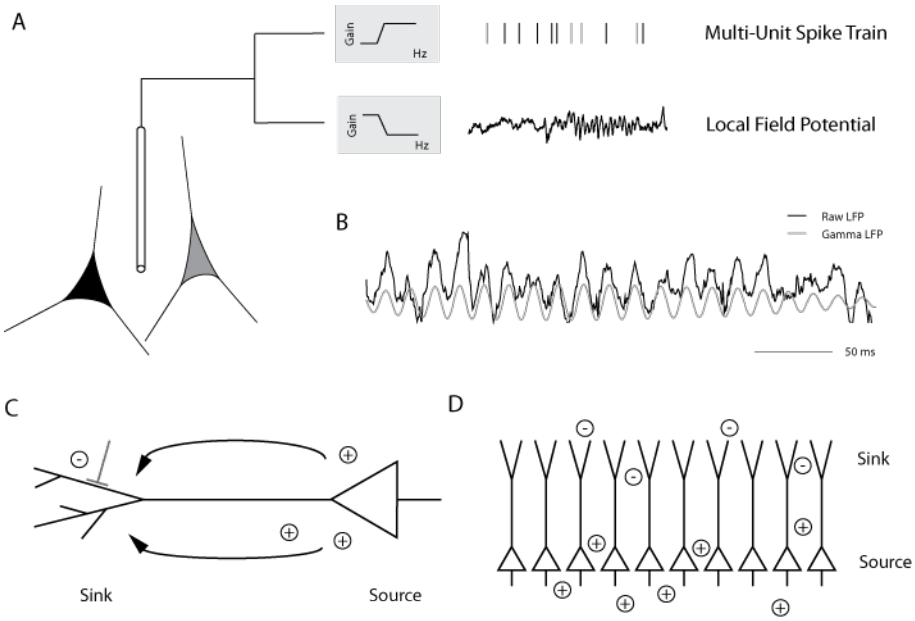

Figure 1. (A) An extracellular electrode placed in the brain measures the mean extracellular field potential, an aggregate signal originating from the population of neurons in the vicinity of the electrode tip. To obtain multi-unit spiking activity, the recorded voltage trace is high-pass filtered and individual action potentials are detected (top). The local field potential (LFP) is comprised of the low frequency components of the extracellular field potential up to 200 Hz (bottom). Its frequency composition varies over time. In the example shown here, prominent oscillations in the frequency band between 30 and 90 Hz – called the gamma-band – are visible during the later part of the trace. (B) In primary visual cortex of awake primates, oscillations in the gamma-band of the LFP are dominant during visual stimulation, as illustrated in the example. The raw signal (black) has been filtered in the gamma frequency range to obtain the gamma LFP (grey). (A) Illustration of a pyramidal cell, where the dendritic tree is shown schematically on the left, the cell body and axon on the right. A synaptic potential creates a current sink on the dendritic tree and a current-source at the soma. Adapted from Johnston and Wu (1995). (B) Pyramidal cells are aligned in a very stereotype fashion, with large dendritic arbours facing one direction and somata facing to the other. In this so-called open field arrangement, synchronized synaptic input creates strong dipoles, since currents flow from individual cells do not cancel each other. Reproduced from Berens et al. (2008).

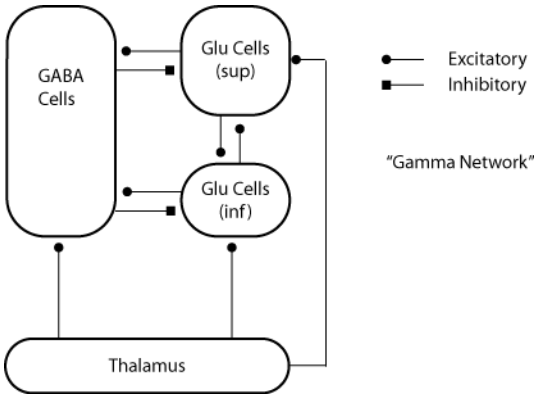

Figure 2. Illustration of the excitatory-inhibitory cortical network involved in the generation of gamma oscillations. Thalamic inputs activate populations of infragranular (inf) and supragranular and granular (sup) glutamergic cells, as well as GABAergic cells. These three groups interact with each other. Inhibitory synapses are indicated by a square, excitatory synapses by a circle. Reproduced from Berens et al. (2008).

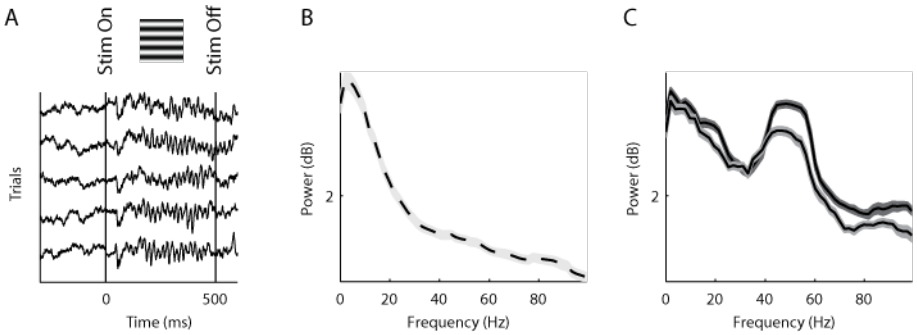

Figure 3. (A) Exemplar raw traces showing the LFP during a typical trial. Before the onset of stimulation, low frequency fluctuations dominate the LFP. During stimulation with an oriented grating, however, strong gamma-oscillations are visible. (B) Typical power spectrum of the LFP during the resting state. Low frequency fluctuations dominate the spectrum, which follows roughly a $1/f$ decay. (C) Typical power spectra of the LFP during visual stimulation with two gratings of different orientation (differing colors). A pronounced power increase in the gamma-band is observed. In particular, this increase depends in strength on the orientation of the visual stimulus. Reproduced from Berens et al. (2008).

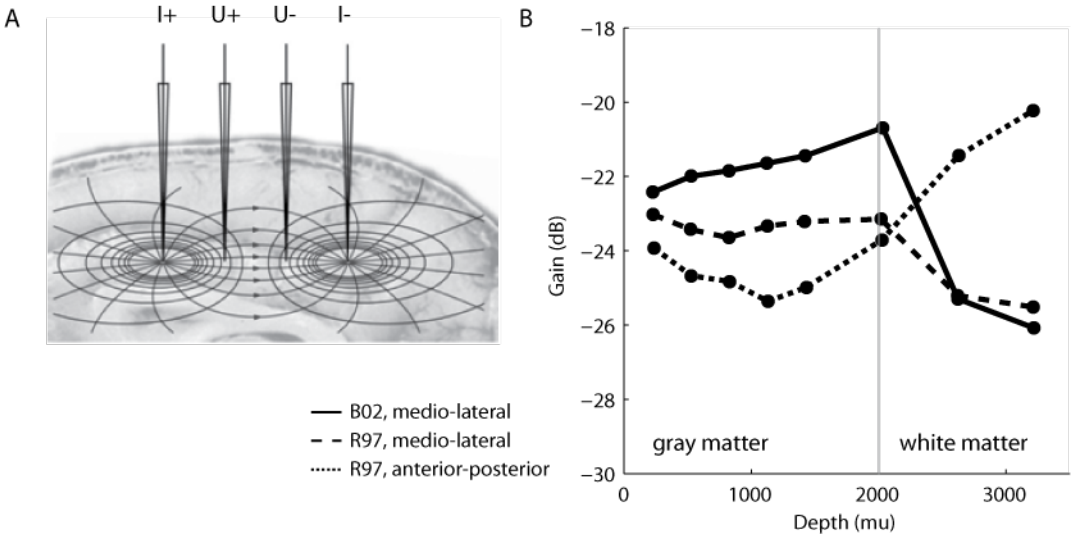

Figure 4. (A) Illustration of the measurement technique for the impedance of the tissue. The current source, driven by a frequency generator, creates a three-dimensional current flow (black lines with arrows) between the two current electrodes (I+ and I-). This current reflects a three-dimensional electric potential (black circles) that leads to a voltage drop across the two measurement electrodes (U+ and U-), which is amplified and measured. The electrodes were placed in the visual cortex using a recording chamber filled with saline. (B) Average impedance (over all frequencies) as a function of cortical depth for three experiments: monkey B02 (solid, measurement direction medio-lateral) and monkey R97 (dashed, medio-lateral; dotted, anterior-posterior). Across cortical depth, the cortical impedance was surprisingly constant. The transition from grey to white matter is marked with a line. Note that the impedance of white matter may be greater or smaller than that of the gray matter, depending on the orientation of the electrode array. Modified from Logothetis et al., Neuron, (2007).

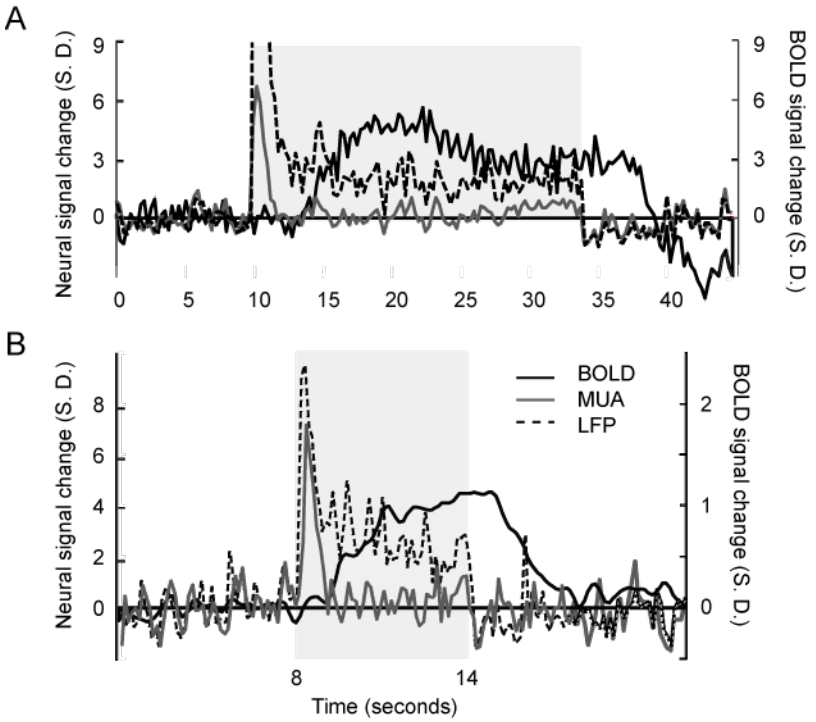

Figure 5. Relationship between BOLD and neurophysiological signals. (A) Responses of multi-unit activity (grey), local field potential (black, dashed) and BOLD (black, solid) under visual stimulation for 24 s (grey background) in an anesthetized macaque. (B) Same as panel A, data was collected in an awake macaque. Modified from Logothetis et al., Nature, 2001 and Goense and Logothetis, Current Biology, 2008, respectively.

Keywords for the index:

Local field potential, LFP, multi-unit activity, microcircuit, BOLD, fMRI, cortical network, open-field arrangement, electric field, interneurons, pyramidal cells, recurrent activity, oscillation, gamma-band, gamma-oscillation, feature selectivity, orientation tuning, spatial resolution of the LFP, dissociation, haemodynamics

References

Abeles M (1991) Corticonics: Neural circuits of the cerebral cortex. Cambridge Univ Pr.

Angelucci A, Bressloff PC (2006) Contribution of feedforward, lateral and feedback connections to the classical receptive field center and extra-classical receptive field surround of primate V1 neurons In Visual Perception - Fundamentals of Vision: Low and Mid-Level Processes in Perception Elsevier, p. 93-120. Available at: http://www.sciencedirect.com/science/article/B7CV6-4M0C546-9/2/bae4b6e3c77e60bb9cf863accb4e7cb1 [Accessed August 15, 2008].

Angelucci A, Sainsbury K (2006) Contribution of feedforward thalamic afferents and corticogeniculate feedback to the spatial summation area of macaque V1 and LGN. The Journal of Comparative Neurology 498:330-351

Bartfeld E, Grinvald A (1992) Relationships between orientation-preference pinwheels, cytochrome oxidase blobs, and ocular-dominance columns in primate striate cortex. Proceedings of the National Academy of Sciences of the United States of America 89:11905–11909

Bartos M, Vida I, Jonas P (2007) Synaptic mechanisms of synchronized gamma oscillations in inhibitory interneuron networks. Nat Rev Neurosci 8:45-56

Bedard C, Kroger H, Destexhe A (2006) Does the 1/f Frequency Scaling of Brain Signals Reflect Self-Organized Critical States? Phys. Rev. Lett. 97:118102-4

Bédard C, Destexhe A (2009) Macroscopic Models of Local Field Potentials and the Apparent 1/f Noise in Brain Activity. Biophysical Journal 96:2589-2603

Belitski A, Gretton A, Magri C, Murayama Y, Montemurro MA, Logothetis NK, Panzeri S (2008) Low-Frequency Local Field Potentials and Spikes in Primary Visual Cortex Convey Independent Visual Information. J. Neurosci. 28:5696-5709

Berens P, Ecker AS, Hoenselaar A, Siapas AG, Logothetis NK, Tolias AS (2006) Spikes are phase locked to the gamma-band of the
local field potential oscillations in the
primary visual cortex of the macaque In Areadne - Research in Encoding and Decoding of Neural Ensembles Santorini, p. p. 46. Available at: http://www. areadne.org/2006/pezaris-hatsopoulos-2006-areadne.pdf.

Berens P, Keliris GA, Ecker AS, Logothetis NK, Tolias AS (2008a) Feature selectivity of the gamma-band of the local field potential in primate primary visual cortex. Front Neurosci 2:199-207

Berens P, Keliris GA, Ecker AS, Logothetis NK, Tolias AS (2008b) Comparing the feature selectivity of the gamma-band of the local field potential and the underlying spiking activity in primate visual cortex. Frontiers in Systems Neuroscience 2 Available at: http://www.frontiersin.org/systemsneuroscience/paper/10.3389/neuro.06/002.2008/html/ [Accessed July 15, 2008].

Besserve M, Schölkopf B, Logothetis N, Panzeri S (2010) Causal relationships between frequency bands of extracellular signals in visual cortex revealed by an information theoretic analysis. Journal of Computational Neuroscience Available at: http://dx.doi.org/10.1007/s10827-010-0236-5 [Accessed April 19, 2010].

Blasdel GG (1992a) Differential imaging of ocular dominance and orientation selectivity in monkey striate cortex. Journal of Neuroscience 12:3115

Blasdel GG (1992b) Orientation selectivity, preference, and continuity in monkey striate cortex. Journal of Neuroscience 12:3139

Braitenberg V, Schüz A (1998) Cortex: statistics and geometry of neuronal connectivity. Springer Berlin.

Brunel N, Wang X (2003) What Determines the Frequency of Fast Network Oscillations With Irregular Neural Discharges? I. Synaptic Dynamics and Excitation-Inhibition Balance. J Neurophysiol 90:415-430

Buzsáki G (2002) Theta oscillations in the hippocampus. Neuron 33:325–340

Buzsáki G (2004) Large-scale recording of neuronal ensembles. Nature Neuroscience 7:446-451

Buzsaki G, Draguhn A (2004) Neuronal Oscillations in Cortical Networks. Science 304:1926-1929

Cardin JA, Carlen M, Meletis K, Knoblich U, Zhang F, Deisseroth K, Tsai L, Moore CI (2009) Driving fast-spiking cells induces gamma rhythm and controls sensory responses. Nature 459:663-667

Chalk M, Herrero JL, Gieselmann MA, Delicato LS, Gotthardt S, Thiele A (2010) Attention Reduces Stimulus-Driven Gamma Frequency Oscillations and Spike Field Coherence in V1. Neuron 66:114-125

Csicsvari J, Henze DA, Jamieson B, Harris KD, Sirota A, Bartho P, Wise KD, Buzsaki G (2003a) Massively Parallel Recording of Unit and Local Field Potentials With Silicon-Based Electrodes. J Neurophysiol 90:1314-1323

Csicsvari J, Jamieson B, Wise KD, Buzsáki G (2003b) Mechanisms of Gamma Oscillations in the Hippocampus of the Behaving Rat. Neuron 37:311-322

David SV, Malaval N, Shamma SA (2010) Decoupling Action Potential Bias from Cortical Local Field Potentials. Computational Intelligence and Neuroscience 2010:1-13

DeFelipe J (1997) Types of neurons, synaptic connections and chemical characteristics of cells immunoreactive for calbindin-D28K, parvalbumin and calretinin in the neocortex. Journal of Chemical Neuroanatomy 14:1–19

Destexhe A, Contreras D, Steriade M (1999) Spatiotemporal Analysis of Local Field Potentials and Unit Discharges in Cat Cerebral Cortex during Natural Wake and Sleep States. J. Neurosci. 19:4595-4608

Douglas RJ, Martin KA (2004) Neuronal circuits of the neocortex.

Douglas RJ, Martin KA (1991) A functional microcircuit for cat visual cortex. The Journal of Physiology 440:735

Frien A, Eckhorn R, Bauer R, Woelbern T, Gabriel A (2000) Fast oscillations display sharper orientation tuning than slower components of the same recordings in striate cortex of the awake

monkey. Eur. J. Neurosci 12:1453-65

Fries P (2009) Neuronal Gamma-Band Synchronization as a Fundamental Process in Cortical Computation. Annual Review of Neuroscience 32:209-224

Fries P, Neuenschwander S, Engel AK, Goebel R, Singer W (2001) Rapid feature selective neuronal synchronization through correlated latency shifting. Nat Neurosci 4:194-200

Fries P, Nikolic D, Singer W (2007) The gamma cycle. Trends in Neurosciences 30:309-316

Fries P, Reynolds JH, Rorie AE, Desimone R (2001) Modulation of Oscillatory Neuronal Synchronization by Selective Visual Attention. Science 291:1560-1563

Fries P, Womelsdorf T, Oostenveld R, Desimone R (2008) The Effects of Visual Stimulation and Selective Visual Attention on Rhythmic Neuronal Synchronization in Macaque Area V4. J. Neurosci. 28:4823-4835

Gail A, Brinksmeyer HJ, Eckhorn R (2004) Perception-related Modulations of Local Field Potential Power and Coherence in Primary Visual Cortex of Awake Monkey during Binocular Rivalry. Cereb. Cortex 14:300-313

Gerwinn S, Berens P, Bethge M (2009) A joint maximum-entropy model for binary neural population patterns and continuous signals In Proceedings of the Twenty-Third Annual Conference on Neural Information Processing Systems MIT Press, p. 620-628.

Gieselmann MA, Thiele A (2008) Comparison of spatial integration and surround suppression characteristics in spiking activity and the local field potential in macaque V1. European Journal of Neuroscience 28:447-459

Goense JB, Logothetis NK (2008) Neurophysiology of the BOLD fMRI Signal in Awake Monkeys. Current Biology Vol 18:631-640

Gray CM, Maldonado PE, Wilson M, McNaughton B (1995) Tetrodes markedly improve the reliability and yield of multiple single-unit isolation from multi-unit recordings in cat striate cortex. Journal of Neuroscience Methods 63:43–54

Hasenstaub A, Shu Y, Haider B, Kraushaar U, Duque A, McCormick* DA (2005) Inhibitory Postsynaptic Potentials Carry Synchronized Frequency Information in Active Cortical Networks. Neuron Vol 47:423-435

Henrie JA, Shapley R (2005) LFP Power Spectra in V1 Cortex: The Graded Effect of Stimulus Contrast. J Neurophysiol 94:479-490

Henze DA, Borhegyi Z, Csicsvari J, Mamiya A, Harris KD, Buzsaki G (2000) Intracellular Features Predicted by Extracellular Recordings in the Hippocampus In Vivo. J Neurophysiol 84:390-400

Hubel DH, Wiesel TN (1974) Sequence regularity and geometry of orientation columns in the monkey striate cortex. J Comp Neurol 158:267-93

Hubel DH, Wiesel TN (1968) Receptive fields and functional architecture of monkey striate cortex. The Journal of Physiology 195:215-243

Johnston D, Wu SM (1995) Foundations of cellular neurophysiology. MIT press Cambridge, MA.

Juergens E, Guettler A, Eckhorn R (1999) Visual stimulation elicits locked and induced gamma oscillations in monkey intracortical- and EEG-potentials, but not in human EEG. Experimental Brain Research 129:247-259

Kamondi A, Acsady L, Wang X, Buzsaki G (1998) Theta oscillations in somata and dendrites of hippocampal pyramidal cells in vivo: Activity-dependent phase-precession of action potentials. Hippocampus 8:244-261

Kang K, Shelley M, Henrie J, Shapley R (2010) LFP spectral peaks in V1 cortex: network resonance and cortico-cortical feedback. Journal of Computational Neuroscience in press Available at: http://dx.doi.org/10.1007/s10827-009-0190-2 [Accessed December 22, 2009].

Katzner S, Nauhaus I, Benucci A, Bonin V, Ringach DL, Carandini M (2009) Local Origin of Field Potentials in Visual Cortex. Neuron 61:35-41

Kayser C, Kim M, Ugurbil K, Kim D, Konig P (2004) A Comparison of Hemodynamic and Neural Responses in Cat Visual Cortex Using Complex Stimuli. Cereb. Cortex 14:881-891

Kayser C, König P (2004) Stimulus locking and feature selectivity prevail in complementary frequency ranges of V1 local field potentials. Eur J Neurosci 19:485-9

Kayser C, Petkov CI, Logothetis NK (2007) Tuning to Sound Frequency in Auditory Field Potentials. J Neurophysiol 98:1806-1809

Kelly R, Smith M, Kass R, Lee T (2010) Local field potentials indicate network state and account for neuronal response variability. Journal of Computational Neuroscience in press Available at: http://dx.doi.org/10.1007/s10827-009-0208-9 [Accessed January 26, 2010].

Khawaja FA, Tsui JMG, Pack CC (2009) Pattern Motion Selectivity of Spiking Outputs and Local Field Potentials in Macaque Visual Cortex. J. Neurosci. 29:13702-13709

Kreiman G, Hung CP, Kraskov A, Quiroga RQ, Poggio T, DiCarlo JJ (2006) Object Selectivity of Local Field Potentials and Spikes in the Macaque Inferior Temporal Cortex. Neuron 49:433-445

Lauritzen M, Gold L (2003) Brain Function and Neurophysiological Correlates of Signals Used in Functional Neuroimaging. J. Neurosci. 23:3972-3980

Lee S, Sen K, Kopell N (2009) Cortical Gamma Rhythms Modulate NMDAR-Mediated Spike Timing Dependent Plasticity in a Biophysical Model. PLoS Comput Biol 5:e1000602

Levitt JB, Lund JS (2002) The spatial extent over which neurons in macaque striate cortex pool visual signals. Vis Neurosci 19:439-52

Linden H, Pettersen K, Einevoll G (2010) Intrinsic dendritic filtering gives low-pass power spectra of local field potentials. Journal of Computational Neuroscience submitted

Linden H, Pettersen K, Tetzlaff T, Potjans T, Denker M, Diesmann M, Grun S, Einevoll G (2009) Estimating the spatial range of local field potentials in a cortical population model. BMC Neuroscience 10:P224

Liu J, Newsome WT (2006) Local Field Potential in Cortical Area MT: Stimulus Tuning and Behavioral Correlations. J. Neurosci. 26:7779-7790

Logothetis NK (2003) MR imaging in the non-human primate: studies of function and of dynamic connectivity. Current Opinion in Neurobiology 13:630-642

Logothetis NK (2007) The ins and outs of fMRI signals. Nat Neurosci 10:1230-1232

Logothetis NK (2003) The Underpinnings of the BOLD Functional Magnetic Resonance Imaging Signal. J. Neurosci. 23:3963-3971

Logothetis NK (2008) What we can do and what we cannot do with fMRI. Nature 453:869-878

Logothetis NK, Kayser C, Oeltermann A (2007) In Vivo Measurement of Cortical Impedance Spectrum in Monkeys: Implications for Signal Propagation. Neuron 55:809-823

Logothetis NK, Pauls J, Augath M, Trinath T, Oeltermann A (2001) Neurophysiological investigation of the basis of the fMRI signal. Nature 412:150-157

Lund JS, Yoshioka T, Levitt JB (1994) Substrates for Interlaminar Connections in Area VI of Macaque Monkey Cerebral Cortex. Cerebral Cortex: Primary Visual Cortex in Primates:37

Lund JS, Angelucci A, Bressloff PC (2003) Anatomical Substrates for Functional Columns in Macaque Monkey Primary Visual Cortex. Cereb. Cortex 13:15-24

Magri C, Whittingstall K, Singh V, Logothetis NK, Panzeri S (2009) A toolbox for the fast information analysis of multiple-site LFP, EEG and spike train recordings. BMC Neurosci 10:1-24

Maier A, Adams G, Aura C, Leopold DA (2009) Distinct laminar zones of coherent local field potentials in monkey V1 In Frontiers in Systems Neuroscience. Conference Abstract: Computational and systems neuroscience Salt Lake City.

Makarov V, Makarova J, Herreras O (2010) Disentanglement of local field potential sources by independent component analysis. Journal of Computational Neuroscience in press Available at: http://dx.doi.org/10.1007/s10827-009-0206-y [Accessed January 26, 2010].

Mann EO, Radcliffe CA, Paulsen O (2005) Hippocampal gamma-frequency oscillations: from interneurones to pyramidal cells, and back. J Physiol 562:55-63

Markram H, Toledo-Rodriguez M, Wang Y, Gupta A, Silberberg G, Wu C (2004) Interneurons of the neocortical inhibitory system. Nat Rev Neurosci 5:793-807

Masquelier T, Hugues E, Deco G, Thorpe SJ (2009) Oscillations, Phase-of-Firing Coding, and Spike Timing-Dependent Plasticity: An Efficient Learning Scheme. J. Neurosci. 29:13484-13493

Mazzoni A, Panzeri S, Logothetis NK, Brunel N (2008) Encoding of Naturalistic Stimuli by Local Field Potential Spectra in Networks of Excitatory and Inhibitory Neurons. PLoS Comput Biol 4:e1000239

Mazzoni A, Whittingstall K, Brunel N, Logothetis NK, Panzeri S (2010) Understanding the relationships between spike rate and delta/gamma frequency bands of LFPs and EEGs using a local

cortical network model. NeuroImage in press Available at: http://www.sciencedirect.com/science?_ob=ArticleURL&_udi=B6WNP-4Y05DJ6-5&_user=10&_coverDate=12%2F21%2F2009&_rdoc=33&_fmt=high&_orig=browse&_srch=doc-info(%23toc%236968%239999%23999999999%2399999%23FLA%23display%23Articles)&_cdi=6968&_sort=d&_docanchor=&_ct=171&_acct=C000050221&_version=1&_urlVersion=0&_userid=10&md5=bd58b8d2221e809d2df14478a758134e [Accessed January 2, 2010].

McBain CJ, Fisahn A (2001) Interneurons unbound. Nature Reviews Neuroscience 2:11–23

Miles R, Toth K, Gulyas AI, Hajos N, Freund TF (1996) Differences between somatic and dendritic inhibition in the hippocampus. Neuron 16:815

Mitzdorf U (1985) Current source-density method and application in cat cerebral cortex: investigation of evoked potentials and EEG phenomena. Physiological reviews 65:37

Mitzdorf U (1987) Properties of the evoked potential generators: current source-density analysis of visually evoked potentials in the cat cortex. International Journal of Neuroscience 33:33–59

Moeller S, Freiwald WA, Tsao DY (2008) Patches with Links: A Unified System for Processing Faces in the Macaque Temporal Lobe. Science 320:1355-1359

Murayama Y, Biessmann F, Meinecke FC, Müller K, Augath M, Oeltermann A, Logothetis NK (2010) Relationship between neural and hemodynamic signals during spontaneous activity studied with temporal kernel CCA. Magnetic Resonance Imaging In Press, Corrected Proof Available at: http://www.sciencedirect.com/science/article/B6T9D-4Y6T7WF-2/2/e1590ecf157d365f048405a70d48fb32 [Accessed February 1, 2010].

Nadasdy Z (2009) Information encoding and reconstruction from the phase of action potentials. Front Syst Neurosci 3:6

Niessing J, Ebisch B, Schmidt KE, Niessing M, Singer W, Galuske RAW (2005) Hemodynamic Signals Correlate Tightly with Synchronized Gamma Oscillations. Science 309:948-951

Nir Y, Fisch L, Mukamel R, Gelbard-Sagiv H, Arieli A, Fried I, Malach R (2007) Coupling between Neuronal Firing Rate, Gamma LFP, and BOLD fMRI Is Related to Interneuronal Correlations. Current Biology 17:1275-1285

Nunez PL, Srinivasan R (2006) Electric fields of the brain: the neurophysics of EEG. Oxford University Press, USA.

Panzeri S, Magri C, Logothetis NK (2008) On the use of information theory for the analysis of the relationship between neural and imaging signals. Magnetic Resonance Imaging 26:1015-1025

Pesaran B, Pezaris JS, Sahani M, Mitra PP, Andersen RA (2002) Temporal structure in neuronal activity during working memory in macaque parietal cortex. Nat. Neurosci 5:805-811

Pettersen K, Hagen E, Einevoll G (2008) Estimation of population firing rates and current source densities from laminar electrode recordings. Journal of Computational Neuroscience 24:291-313

Pettersen KH, Einevoll GT (2008) Amplitude Variability and Extracellular Low-Pass Filtering of Neuronal Spikes. Biophysical Journal 94:784-802

Pouille F, Marin-Burgin A, Adesnik H, Atallah BV, Scanziani M (2009) Input normalization by global feedforward inhibition expands cortical dynamic range. Nat Neurosci 12:1577-1585

Ranck Jr JB (1963) Specific impedance of rabbit cerebral cortex. Experimental neurology 7:144

Rasch M, Logthetis NK, Kreiman G (2009) From Neurons to Circuits: Linear Estimation of Local Field Potentials. J. Neurosci. 29:13785-13796

Rasch MJ, Gretton A, Murayama Y, Maass W, Logothetis NK (2008) Inferring Spike Trains From Local Field Potentials. J Neurophysiol 99:1461-1476

Rauch A, Rainer G, Logothetis NK (2008) The effect of a serotonin-induced dissociation between spiking and perisynaptic activity on BOLD functional MRI. Proceedings of the National Academy of Sciences 105:6759-6764

Ray S, Maunsell JH (2009) Gamma oscillations in macaque V1 depend on stimulus characteristics In Society for Neuroscience Meeting Abstract , p. 166.6/V3.

Ray S, Crone NE, Niebur E, Franaszczuk PJ, Hsiao SS (2008a) Neural Correlates of High-Gamma Oscillations (60-200 Hz) in Macaque Local Field Potentials and Their Potential Implications in Electrocorticography. J. Neurosci. 28:11526-11536

Ray S, Hsiao SS, Crone NE, Franaszczuk PJ, Niebur E (2008b) Effect of Stimulus Intensity on the Spike-Local Field Potential Relationship in the Secondary Somatosensory Cortex. J. Neurosci. 28:7334-7343

Rickert J, de Oliveira SC, Vaadia E, Aertsen A, Rotter S, Mehring C (2005) Encoding of Movement Direction in Different Frequency Ranges of Motor Cortical Local Field Potentials. J. Neurosci. 25:8815-8824

Ringach DL, Hawken MJ, Shapley R (1997) Dynamics of orientation tuning in macaque primary visual cortex. Nature 387:281-284

Ringach DL, Shapley RM, Hawken MJ (2002) Orientation Selectivity in Macaque V1: Diversity and Laminar Dependence. J. Neurosci. 22:5639-5651

Sanes JN, Donoghue JP (1993) Oscillations in local field potentials of the primate motor cortex during voluntary movement. Proc Natl Acad Sci USA 90:4470–4474

Scherberger H, Jarvis MR, Andersen RA (2005) Cortical Local Field Potential Encodes Movement Intentions in the Posterior Parietal Cortex. Neuron 46:347-354

Siapas AG, Lubenov EV, Wilson MA (2005) Prefrontal Phase Locking to Hippocampal Theta Oscillations. Neuron 46:141-151

Siegel M, Konig P (2003) A Functional Gamma-Band Defined by Stimulus-Dependent Synchronization in Area 18 of Awake Behaving Cats. J. Neurosci. 23:4251-4260

Sirota A, Montgomery S, Fujisawa S, Isomura Y, Zugaro M, Buzsaki G (2008) Entrainment of Neocortical Neurons and Gamma Oscillations by the Hippocampal Theta Rhythm. Neuron 60:683-697

Sirotin YB, Das A (2008) Anticipatory haemodynamic signals in sensory cortex not predicted by local neuronal activity. Nature 457:475-479

Smith EL, Chino YM, Ridder WH, Kitagawa K, Langston A (1990) Orientation Bias of Neurons in the Lateral Geniculate Nucleus of Macaque Monkeys. Visual Neuroscience 5:525-545

Sohal VS, Zhang F, Yizhar O, Deisseroth K (2009) Parvalbumin neurons and gamma rhythms enhance cortical circuit performance. Nature advanced online publication Available at: http://dx.doi.org/10.1038/nature07991 [Accessed May 22, 2009].

Steriade M (2006) Grouping of brain rhythms in corticothalamic systems. Neuroscience 137:1087-1106

Steriade M, McCormick D, Sejnowski T (1993) Thalamocortical oscillations in the sleeping and aroused brain. Science 262:679-685

Swadlow HA, Gusev AG, Bezdudnaya T (2002) Activation of a Cortical Column by a Thalamocortical Impulse. J. Neurosci. 22:7766-7773

Taylor K, Mandon S, Freiwald W, Kreiter A (2005) Coherent Oscillatory Activity in Monkey Area V4 Predicts Successful Allocation of Attention. Cereb. Cortex 15:1424-1437

Tolias AS, Ecker AS, Siapas AG, Hoenselaar A, Keliris GA, Logothetis NK (2007) Recording Chronically From the Same Neurons in Awake, Behaving Primates. J Neurophysiol 98:3780-3790

Tolias AS, Sultan F, Augath M, Oeltermann A, Tehovnik EJ, Schiller PH, Logothetis NK (2005) Mapping Cortical Activity Elicited with Electrical Microstimulation Using fMRI in the Macaque. Neuron 48:901-911

Trevelyan AJ (2009) The Direct Relationship between Inhibitory Currents and Local Field Potentials. J. Neurosci. 29:15299-15307

Varela F, Lachaux J, Rodriguez E, Martinerie J (2001) The brainweb: Phase synchronization and large-scale integration. Nat Rev Neurosci 2:229-239

Vinck M, Lima B, Womelsdorf T, Oostenveld R, Singer W, Neuenschwander S, Fries P (2010) Gamma-Phase Shifting in Awake Monkey Visual Cortex. J. Neurosci. 30:1250-1257

Viswanathan A, Freeman RD (2007) Neurometabolic coupling in cerebral cortex reflects synaptic more than spiking activity. Nat Neurosci 10:1308-1312

Whittington MA, Traub RD, Jefferys JG (1995) Synchronized oscillations in interneuron networks driven by metabotropic glutamate receptor activation. Nature 373:612–615

Wilke M, Logothetis NK, Leopold DA (2006) Local field potential reflects perceptual suppression in monkey visual cortex. Proc. Natl. Acad. Sci. U.S.A 103:17507-17512

Xing D, Yeh C, Shapley RM (2009) Spatial Spread of the Local Field Potential and its Laminar Variation in Visual Cortex. J. Neurosci. 29:11540-11549

Xu X, Ichida J, Shostak Y, Bonds A, Casagrande V (2002) Are Primate Lateral Geniculate Nucleus (LGN) Cells Really Sensitive to Orientation or Direction? Visual Neuroscience 19:97-108

Young MP, Tanaka K, Yamane S (1992) On oscillating neuronal responses in the visual cortex of the monkey. Journal of Neurophysiology 67:1464

Zhu Y, Stornetta RL, Zhu JJ (2004) Chandelier cells control excessive cortical excitation: characteristics of whisker-evoked synaptic responses of layer⅔ nonpyramidal and pyramidal neurons. Journal of Neuroscience 24:5101